Journal of Vertebrate Paleontology e2118059 (10 pages)

DOI: 10.1080/02724634.2022.2118059

ARTICLE

FIRST RHYNCHOCEPHALIAN (REPTILIA, LEPIDOSAURIA) FROM THE CRETACEOUS–PALEOGENE OF INDIA

S. ANANTHARAMAN, [1,2] DAVID G. DEMAR JR., [3,4,*] R. SIVAKUMAR,[5] DILIP CHANDRA DASSARMA,[2] GREGORY P. WILSON MANTILLA, [3,6] and JEFFREY A. WILSON MANTILLA [7]
[1]Department of Geology, Presidency College, Chennai 600 005, India, gsi_sa@hotmail.com;
[2]Geological Survey of India, Southern Region, dilipchandra@yahoo.com;
[3]Burke Museum, University of Washington, Seattle, Washington, 98195-1800, U.S.A.;
[4]Department of Paleobiology, National Museum of Natural History, Smithsonian Institution, Washington, D.C., 20560, U.S.A., demard@si.edu;
[5]Arignar Anna Govt. Arts College, Villupuram 605 602, India, rsivakumargeology@gmail.com;
[6]Department of Biology, University of Washington, Seattle, Washington, 98195-1800, U.S.A., gpwilson@uw.edu;
[7]Museum of Paleontology and Department of Earth and Environmental Sciences, University of Michigan, Ann Arbor, Michigan, 48109-1085, U.S.A., wilsonja@umich.edu

ABSTRACT—Rhynchocephalia, a once diverse clade of lizard-like reptiles, had a nearly global distribution during much of the Mesozoic. By the Late Cretaceous rhynchocephalians underwent a marked reduction in their diversity and biogeographic range, with sparse records of only deeply nested taxa (e.g., Sphenodontinae) found in the Upper Cretaceous–Paleocene of Patagonia and the Miocene–Recent of New Zealand. Here we describe a partial dentary with teeth of a rhynchocephalian from the Naskal locality, an intertrappean deposit within the Deccan Traps Volcanic Province in peninsular India. This discovery represents the first Cretaceous–Paleogene (K–Pg) record of a rhynchocephalian outside of Patagonia and: (i) demonstrates the clade had a broader Gondwanan distribution during the Cretaceous than previously appreciated and (ii) reinforces the emerging pattern that Rhynchocephalia were confined to Gondwana after the Early Cretaceous. This further extends the rhynchocephalian record in India, which now spans most of the Mesozoic (Late Triassic to ca. K–Pg boundary). The Naskal rhynchocephalian is a member of Acrosphenodontia based on its regionalized, acrodont marginal dentition. Its hatchling teeth appear to be unique (e.g., crowns mesially tipped, distinct break in slope along distal margin) and most similar in morphology to those of *Godavarisaurus lateefi* from the Lower–Middle Jurassic of India. Although the Naskal intertrappean most likely was deposited during the latest Maastrichtian, additional fossil sampling across the K–Pg boundary in India is needed to determine whether the Naskal rhynchocephalian was a victim or survivor of the end-Cretaceous mass extinction.

Citation for this article: Anantharaman, S., D. G. DeMar, Jr., R. Sivakumar, D. C. Dassarma, G. P. Wilson Mantilla, and J. A. Wilson Mantilla. 2022. First rhynchocephalian (Reptilia, Lepidosauria) from the Cretaceous–Paleogene of India. Journal of Vertebrate Paleontology. DOI: 10.1080/02724634.2022.2118059

INTRODUCTION

Rhynchocephalia are a clade of lizard-like reptiles that together with their sister taxon Squamata form crown-group Lepidosauria (Gauthier et al., 1988; de Queiroz and Gauthier, 2020). Whereas Squamata today comprise over 11,000 species globally (Uetz et al., 2022), Rhynchocephalia include only the tuatara (*Sphenodon punctatus*), which is restricted to New Zealand (Cree, 2014). The striking contrast in the diversity and geographic distribution of modern rhynchocephalians and squamates is the product of a deep Mesozoic history that extends to at least the Middle Triassic, when the first rhynchocephalians are recorded (Jones et al., 2013). By the Late Triassic, Rhynchocephalia achieved a nearly global distribution (Jones et al., 2009), and by the Cretaceous were both diverse in body form and size and had occupied multiple habitats (see below). Available records suggest that much of this distribution had diminished by the early Cenozoic to a small region of South America (Apesteguía et al., 2014), and possibly Antarctica/New Zealand (Apesteguía and Jones, 2012). The rhynchocephalian range contraction might have been related to the global expansion of modern lizard clades (e.g., Jones, 2006a, 2013; Herrera-Flores et al., 2021), expansion/contraction of preferred environments (Evans, 1995, 1998; Rauhut et al., 2012), or both.

The general geographic pattern of expansion and contraction of Rhynchocephalia parallels that of their taxonomic and ecomorphological diversity. During much of the Mesozoic rhynchocephalians were diverse (e.g., Jones, 2006a, 2006b, 2008, 2009; Jones et al., 2009), including small, gracile, terrestrial insectivores (e.g., *Gephyrosaurus*; Evans, 1980, 1981), large, robust, terrestrial herbivores (e.g., *Priosphenodon*; Apesteguía and Novas, 2003; LeBlanc et al., 2020), and aquatic forms with elongate bodies and short limbs (e.g., *Pleurosaurus*; Carroll, 1985). Peak taxonomic richness occurred during the Late Triassic (> 22 named species in 11 genera) and Late Jurassic (> 18 named species in 14 genera; paleobiodb.org, accessed 5 February 2022). In the Early Cretaceous, rhynchocephalian diversity declined to only about eight species, with fewer records in North and South America, Europe, and South Africa (e.g., Throckmorton et al., 1981; Evans and Sigogneau-Russell, 1997; Reynoso, 1997, 2000; Evans et al., 2001; Apesteguía and Carballido, 2014; Cau et al.,

*Corresponding author
Color versions of one or more of the figures in the article can be found online at www.tandfonline.com/ujvp.

Published online 26 Sep 2022

2014). By the end of the Late Cretaceous, there were only two rhynchocephalian species, both from the upper Campanian–lower Maastrichtian of Argentina: *Kawasphenodon expectatus* from the Los Alamitos Formation (Apesteguía, 2005) and *Lamarquesaurus cabazai* from the Allen Formation (Apesteguía and Rougier, 2007). Other unnamed taxa from the same geologic units are based on highly incomplete material and may not be taxonomically distinct from *K. expectatus* and *L. cabazai* (Martinelli and Forasiepi, 2004; Apesteguía, 2005). The spatial contraction and drop in diversity of rhynchocephalians may have been accompanied by a decline in evolutionary rates (Simões et al., 2020).

The Cenozoic record of Rhynchocephalia is limited to a few southern landmasses. *Kawasphenodon peligrensis* from the Paleocene of Patagonia represents the only rhynchocephalian genus known to have survived the Cretaceous–Paleogene (K–Pg) mass extinction ca. 66 million years ago (Apesteguía et al., 2014; see Augé and Rage, 2006, for a tentative rhynchocephalian record from the Paleocene of Morocco). After an approximately 40 Ma gap, Rhynchocephalia reappeared in the Miocene–late Pleistocene of New Zealand, where the clade today is represented by a single species, *Sphenodon punctatus* (e.g., Jones et al., 2009; Cree, 2014).

The record of Rhynchocephalia in India (Fig. 1A) mirrors their global record, with occurrences concentrated in the early part of the Mesozoic. Records from the Upper Triassic (Carnian–Norian) Tiki Formation are highly incomplete and include an indeterminate rhynchocephalian represented by a partial maxilla with teeth (Ray et al., 2016:fig. 7f–h) and two other tooth-bearing elements that, in our opinion, are not unequivocally rhynchocephalian (see Ray et al., 2016:fig. 7I; Jitendra and Milankumar, 2019:pl. I, figs. 5–8). The long and slender dentary identified by Ray et al. (2016) as a possible new rhynchocephalian is more similar to that of the Late Triassic lepidosauromorph *Sophineta cracoviensis* (Evans and Borsuk-Białynicka, 2009:fig. 8) than it is to basally diverging rhynchocephalians (e.g., *Gephyrosaurus bridensis*, Evans, 1980; *Diphydontosaurus avonis*, Whiteside, 1986) in its deeply pleurodont tooth attachment, continuous tooth replacement, and moderately spaced, tall, slender, conical teeth, and dorsally positioned dentary symphysial articulatory surface. Other putative Tiki records include undescribed and unfigured sphenodontian teeth (Datta et al., 2004). Unambiguous rhynchocephalian specimens from the Lower–Middle Jurassic Kota Formation (*Rebbanosaurus jaini* and *Godavarisaurus lateefi*; Evans et al., 2001) are more abundant, better preserved, and complete enough to incorporate into phylogenetic analyses, where they are commonly recovered outside Eusphenodontia: the clade that includes clevosaurs, pleurosaurs, saphaeosaurs, eilenodontines, and sphenodontines (e.g., Apesteguía et al., 2012; Herrera-Flores et al., 2018; Romo de Vivar et al., 2020; Simões et al., 2020, 2022; DeMar et al., in press). A possible third rhynchocephalian from the Kota Formation, *Bharatagama rebbanensis*, was originally considered an acrodontan iguanian (Evans et al., 2002), but it was recently hypothesized to be a rhynchocephalian (Conrad, 2018).

Here we describe the first rhynchocephalian occurrence from the Cretaceous–Paleogene of India, which represents the only such record outside of Patagonia. The specimen, a partial dentary with teeth, is from the Naskal intertrappean locality in the south-central state of Telangana in peninsular India. The Naskal taxon is an acrosphenodontian and most similar morphologically to *Godavarisaurus*. The presence of the Naskal taxon is consistent with Rhynchocephalia being found only on the southern landmasses after the Early Cretaceous and has implications for the K–Pg mass extinction.

Institutional Abbreviations—**GSI/PAL/SR**, Geological Survey of India, Palaeontology Division, Southern Region, Hyderabad, India; **VPL/JU/KR**, Kota Reptile Collection, Vertebrate Palaeontology, University of Jammu, India.

MATERIALS AND METHODS

Measurements

Measurements are straight-line values taken from high-resolution digital images in ImageJ 1.53c (imagej.nih.gov/ij/). The digital images were captured using a Leica MZ9.5 binocular dissecting microscope, with Clemex imaging hardware and software including Captiva Entry-Level Image Analysis v. 7.0.700.

Microcomputed Tomography

GSI/SR/PAL-NR-0101 was scanned using a Bruker SkyScan 1172 Micro-CT scanner for virtual 3D reconstruction at a resolution of 8.21740 µm and with a source voltage and current of 48 kV and 208 uA, respectively. GSI/SR/PAL-NR-0101 was segmented and volumetrically 3D rendered in 3D Slicer v. 4.6.2 and 4.11.0 (slicer.org).

Anatomical Terminology and Clade Definitions

The anatomical terminology used here primarily follows Robinson (1976), Evans et al. (2001), and Apesteguía et al. (2012). The marginal dentition of most rhynchocephalians that are more deeply nested than *Diphydontosaurus avonis* (i.e., Acrosphenodontia as defined in Chambi-Trowell et al., 2021) is divided into three regions of acrodont teeth. These include (i) the immature hatchling teeth that typically alternate in size, (ii) the mesially positioned, more mature successional teeth that in some taxa become enlarged and caniniform (e.g., *Sphenodon punctatus*), and (iii) the additional teeth, which are added one by one behind the hatchling series as the jaw grows (Robinson, 1976; Reynoso, 2003).

Clade names used herein follow the definitions presented in Chambi-Trowell et al. (2021).

GEOLOGICAL AND PALEONTOLOGICAL SETTING

Exposures of volcano-sedimentary rocks of the southeastern part of the main Deccan Traps Volcanic Province (DTVP) occur in the Vikarabad District of Telangana State, about 70 km west of Hyderabad. Detailed geological mapping of the area and its surroundings (Dutt, 1975) has identified nine volcanic flows and four intervening "intertrappean" sedimentary deposits. This volcano-sedimentary sequence overlies either Precambrian Bhima Group rocks or Archean gneisses and granites. The intertrappean section that yielded the fossil described herein is located about 2 km northeast of the village of Naskal (17°14′21′′N, 77°53′16′′E; Wilson Mantilla et al., 2022:figs. 1, 3–5; Fig. 1A). This ~2.7 m thick section was deposited between flows "3a" and "4" of the Deccan Traps and comprises mudstones, shales, cherts, limestones, marlstones, and clays (Wilson Mantilla et al., 2022:fig. 5; Fig. 1B). In the 1990s, a team led by the Geological Survey of India (GSI), Southern Region collected ~18,000 kg of bulk sediment from multiple units in this section. Underwater screen-washing of samples from the ~30 cm thick white marlstone to mudstone unit has yielded a rich vertebrate microfossil assemblage of ~3,000 specimens, including a variety of fish jaws, teeth, and otoliths, anuran postcranial elements, squamate vertebrae, turtle shell, crocodilian teeth, and mammalian teeth, incomplete jaws, and postcranial elements (e.g., Das Sarma et al., 1995; Anantharaman and Das Sarma, 1997; Wilson et al., 2007; Wilson Mantilla et al., 2022). No definitive dinosaur specimens have been reported from our Naskal collections or those from other workers (e.g., Prasad and Sahni, 1988; Khajuria and

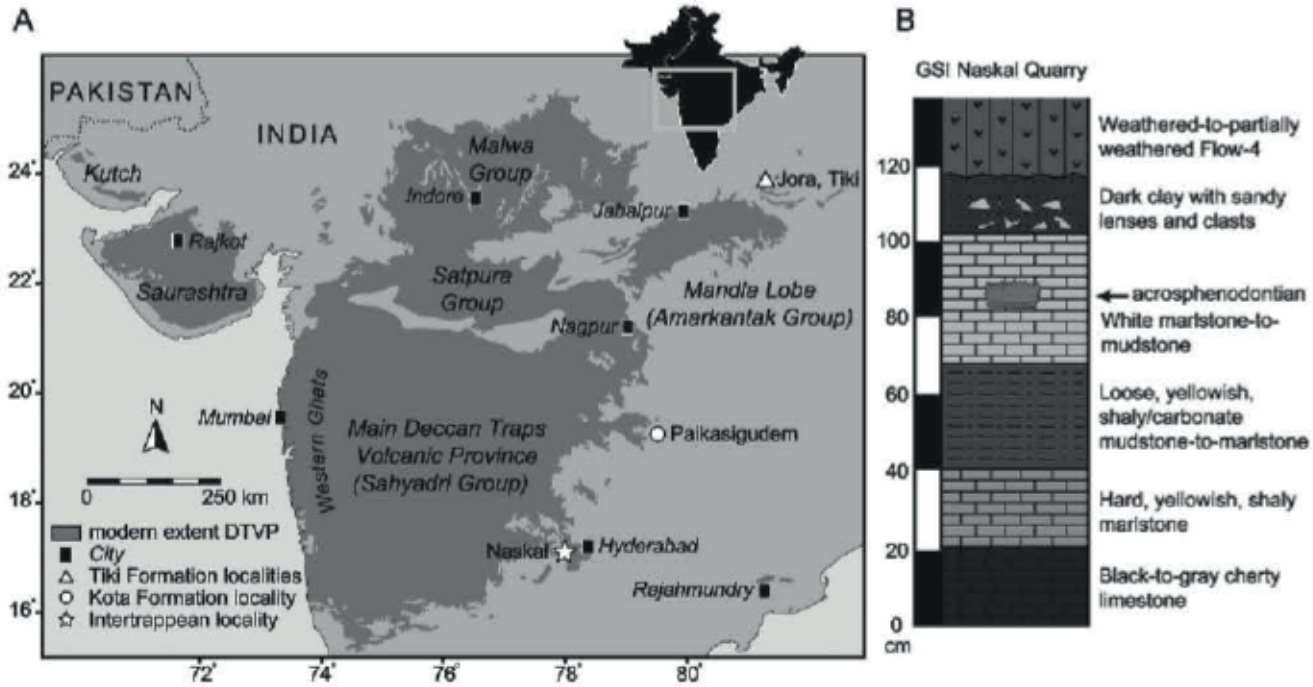

FIGURE 1. A, map of India showing geographic positions of fossil rhynchocephalian localities from the Tiki (Upper Triassic) and Kota (Lower–Middle Jurassic) formations and the Naskal Intertrappean locality (uppermost Cretaceous/lowermost Paleocene); B, sedimentological log of the Geological Survey of India (GSI) Naskal Quarry. **Abbreviation: DTVP**, Deccan Traps Volcanic Province. The map and tracing of the DTVP are modified from Wilson et al. (2019: fig. 1) and Wilson Mantilla et al. (2022:fig. 1). The sedimentological log is modified from Wilson Mantilla et al. (2022:fig. 5, top right).

Prasad, 1998; Prasad, 2012). Wilson Mantilla et al. (2022) provided more geological details, reviewed evidence for the age of the locality, and presented new $^{40}Ar/^{39}Ar$ data that indicate a most probable latest Cretaceous age for the site (66.136–66.056 Ma), but an earliest Paleocene age cannot be ruled out. Note that the geographic coordinates for the Naskal locality provided here and in the "Geological setting" and fig. 3 of Wilson Mantilla et al. (2022) are correct, but those in the "Systematic Paleontology" section of Wilson Mantilla et al. (2022) are incorrect.

SYSTEMATIC PALEONTOLOGY

LEPIDOSAURIA Haeckel, 1866 sensu Evans, 1984
RHYNCHOCEPHALIA Günther, 1867 sensu Gauthier, Estes, and de Queiroz, 1988
SPHENODONTIA Williston, 1925 sensu Chambi-Trowell, Martinelli, Whiteside, Romo de Vivar, Soares, Schultz, Gill, Benton, and Rayfield, 2021
ACROSPHENODONTIA Chambi-Trowell, Martinelli, Whiteside, Romo de Vivar, Soares, Schultz, Gill, Benton, and Rayfield, 2021
ACROSPHENODONTIA indet.
(Figs. 2, 3)

Referred Specimen—A partial right dentary with teeth (GSI/SR/PAL-NR-0101).

Locality and Horizon—The locality is near Naskal, Telangana, India (17°14′21″N, 77°53′16″E; Fig. 1A). Fossils were found in the white marlstone to mudstone below the dark clay with sandy lenses and clasts and above the loose, yellowish, shaly/carbonate mudstone to marlstone at the GSI Naskal quarry (Fig. 1B). Application of Monte Carlo methods and Bayesian constraint to $^{40}Ar/^{39}Ar$ ages of the bounding lavas (Wilson Mantilla et al., 2022) indicates that the permissible age range of the Naskal intertrappean is between 66.136 and 66.056 Ma, at 68% confidence. Additional data are available from Wilson Mantilla et al. (2022) and the GSI.

DESCRIPTION

GSI/SR/PAL-NR-0101 is an anterior portion of a right dentary with nine partial to complete teeth (Figs. 2, 3). The maximum preserved length and height of the specimen (excluding the teeth) is 2.9 mm and 1.2 mm, respectively. The complete dentary might have been up to 10 mm long. The symphysis is not preserved. The jaw is gracile, with its greatest mediolateral width approximately 6.5% of its estimated total length.

Portions of the surface of the bone and some of the teeth are pitted and corroded (e.g., Fig. 3E–G), a condition typical of many of the mammal teeth found at the Naskal locality (e.g., Prasad and Sahni, 1988; Prasad et al., 1994; Wilson Mantilla et al., 2022). This pitting might have been the result of the physical and chemical processes of pedogenesis at the Naskal locality (Khajuria and Prasad, 1998) or digestive corrosion by carnivore gastric fluids (e.g., Smith et al., 2021).

Dentary

Dentary GSI/SR/PAL-NR-0101 is elongate in dorsal view (Fig. 2C). Its lateral margin is nearly straight, and its medial margin is broadly concave. The tooth-bearing portion of the dentary widens posteriorly to accommodate the larger distal teeth, and, along that surface, the teeth become increasingly offset lingually. The three smallest teeth are positioned in line with the labial half of the larger teeth. The ventral margin of the dentary is broadly convex in transverse section, and its surface is smooth, with

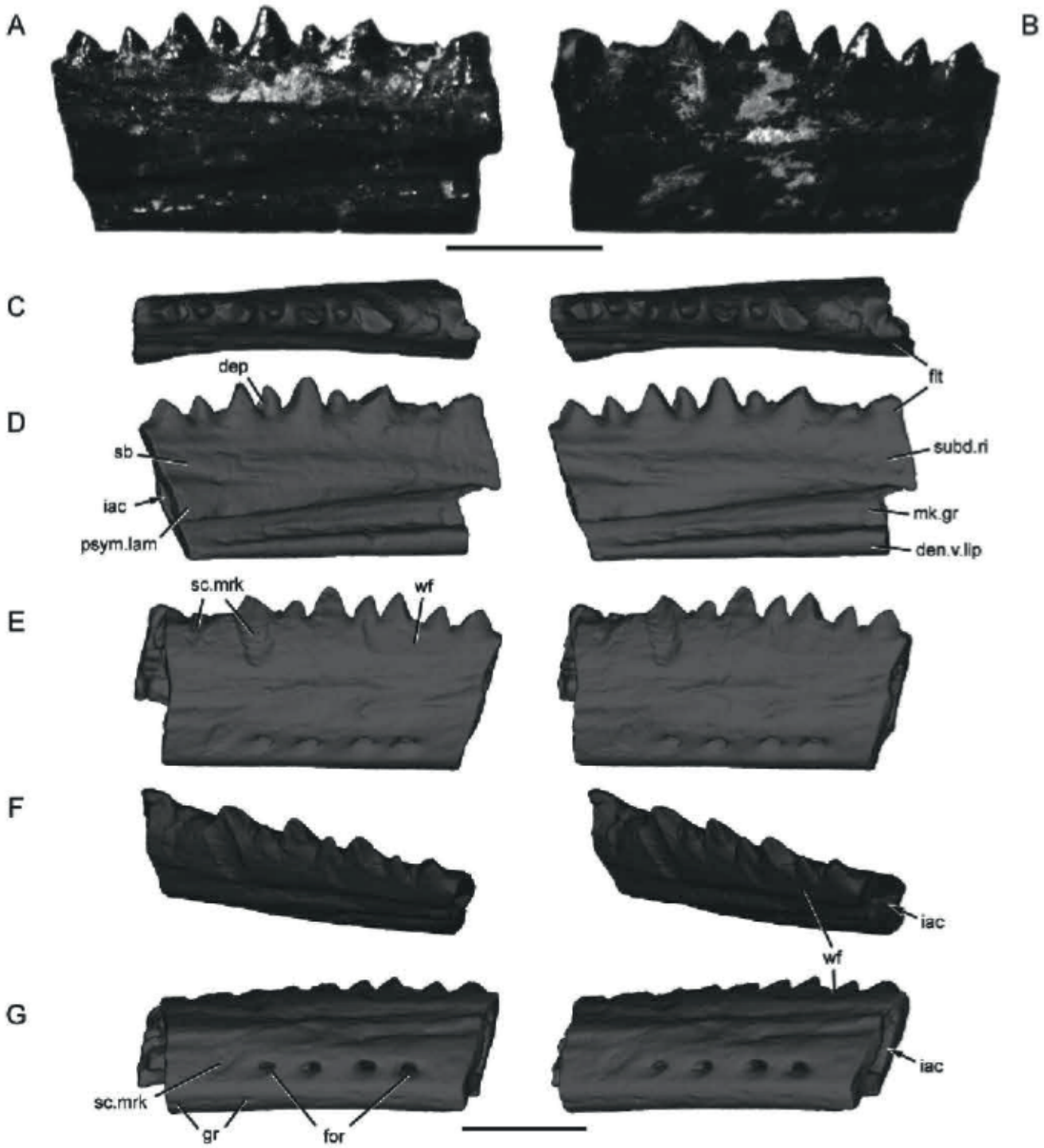

FIGURE 2. Digital photographs and virtual 3D renderings of the right dentary (GSI/SR/PAL-NR-0101) of an indeterminate acrosphenodontian from the Naskal locality, central India. **A**, **B**, digital photographs in **A**, medial and **B**, lateral views. **C–G**, virtual 3D stereopairs in **C**, dorsal, **D**, medial, **E**, lateral, **F**, oblique anterolateral and dorsal, and **G**, ventrolateral views. **Abbreviations**: **den.v.lip**, ventral lip of the dentary; **dep**, depression; **flt**, flattened surface; **for**, foramen; **gr**, groove; **iac**, inferior alveolar canal; **mk.gr**, Meckelian groove; **psym.lam**, postsymphyseal lamina; **sb**, strip of secondary bone; **sc.mrk**, scour mark; **subd.ri**, subdental ridge; **wf**, wear facet. All scale bars equal 1 mm.

several faint, mediolaterally narrow grooves that extend a short distance anteroposteriorly (Fig. 2G).

In medial view, the subdental ridge is moderately deep dorsoventrally and deepest at the preserved anterior extreme of the jaw (Fig. 2A, D). A thickened strip of secondary bone extends obliquely across the medial surface of the subdental ridge (Figs. 2A, D, 3E). The surface of the dentary is shallowly concave above this strip of secondary bone, with weak linear and crescent-shaped ridges (Figs. 2A, 3E); there is no indication of occlusal wear from the palatine dentition on this surface.

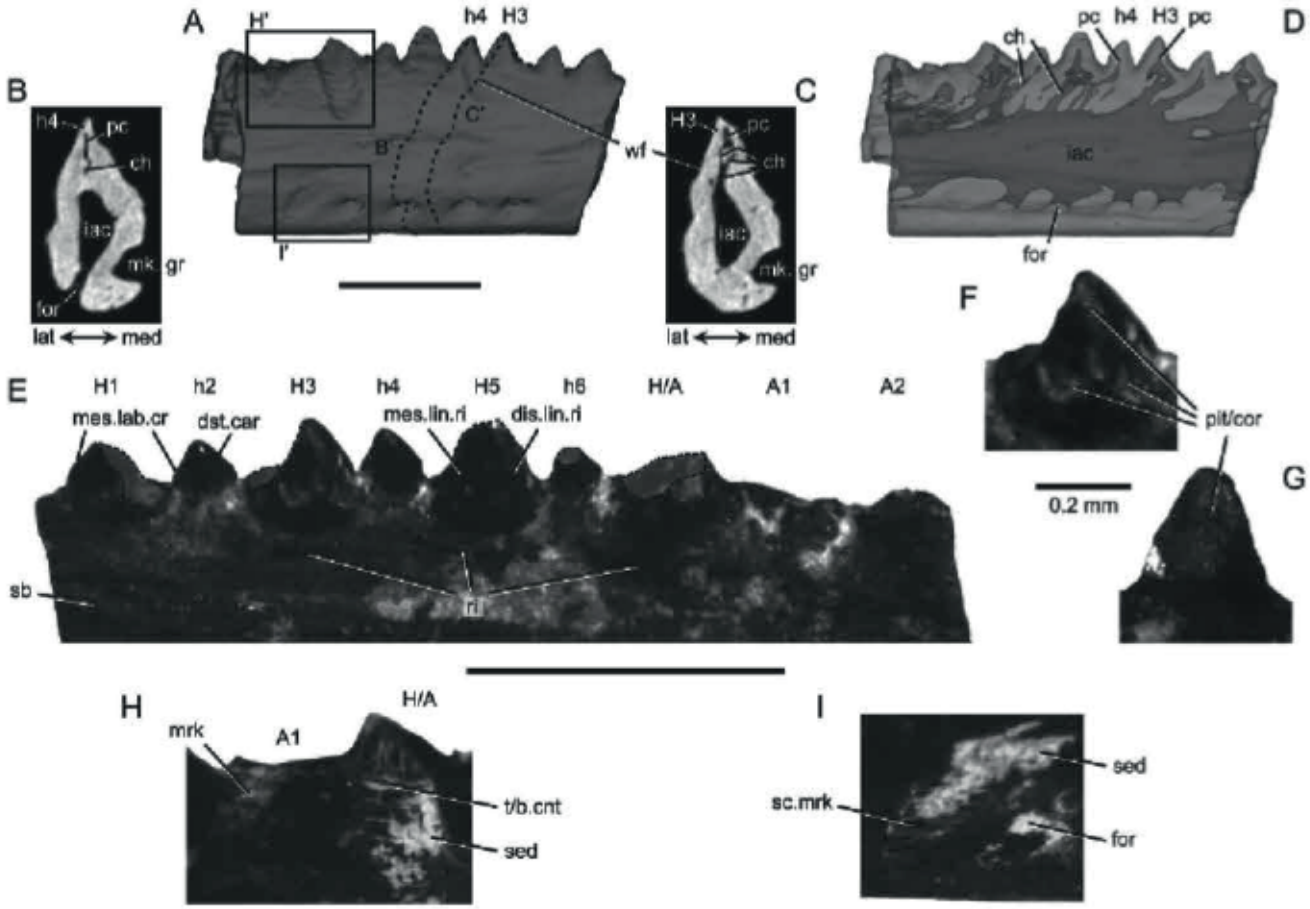

FIGURE 3. External and internal features of the right dentary and its teeth (GSI/SR/PAL-NR-0101) of an indeterminate acrosphenodontian from the Naskal locality, central India. **A**, virtual 3D rendering in lateral view showing location of the oblique coronal sections B' and C' (dashed lines) of the μCT slices shown in **B** and **C**, respectively. Black boxes H' and I' delimit the region of the jaw shown enlarged at **H** and **I**, respectively. **B, C**, μCT slice images. **D**, 70% transparent, virtual 3D rendering in lateral view showing the internal pulp cavities and the channel(s) that connect them to the inferior alveolar canal. **E**, digital image of the dentary teeth in lingual and slight occlusal views; the dashed lines filled with 50% transparent gray indicate the broken portions of the better-preserved teeth. **F**, hatchling tooth 'H3' oriented as in **E** showing pitted/corroded tooth enamel. **G**, hatchling tooth 'H5' in labial view showing large pitted/corroded surface. **H**, closeup of the two dorsolateral marks adjacent teeth H/A and A1. **I**, closeup of the ventrolateral scour mark. **Abbreviations: A**, additional teeth; **ch**, channel; **dst.car**, distal carina; **dis.lin.ri**, distolingual ridge; **for**, foramen; **H**, large hatchling tooth; **h**, small hatchling tooth; **H/A**, distalmost hatchling or mesialmost additional tooth; **iac**, inferior alveolar canal; **lat**, lateral; **med**, medial; **mes.lab.cr**, mesiolabial crest; **mes.lin.ri**, mesiolingual ridge; **mk.gr**, Meckelian groove; **mrk**, undetermined taphonomic mark; **pc**, pulp cavity; **pit/cor**, pitted/corroded surface; **ri**, ridge; **sb**, strip of secondary bone; **sc.mrk**, scour mark; **sed**, sediment; **t/b.cnt**, tooth/bone contact; **wf**, wear facet. Scale bars equal 1 mm, except where noted.

Below this strip of secondary bone, the postsymphyseal lamina is triangular and tapers posteriorly (Fig. 2A, D). Anteriorly, a shallow groove extends the length of the first three tooth positions along the contact between the postsymphyseal lamina and secondary bone. Within the lower half of the dentary, the Meckelian groove deepens posteriorly in both dorsoventral and mediolateral directions. It is bordered dorsally by the subdental ridge/postsymphyseal lamina and ventrally by the ventral lip of the dentary (Fig. 2A, D). The Meckelian groove opens medially and trends slightly anteroventrally, such that its ventral margin approaches the ventral lip of the dentary anteriorly. No splenial facets are apparent along the preserved portions of the upper and lower margins of the Meckelian groove, which likely indicates the absence of that bone (a synapomorphy of Rhynchocephalia; Gauthier et al., 1988). Similarly, no angular facet is present on the ventral lip of the dentary, which indicates that the jaw was broken anterior to the angular articulation with the dentary.

The ventral margin of the dentary is straight in lateral view, whereas the dorsal margin appears slightly convex; as preserved, there is no apparent anterior or posterior tapering of the jaw (Fig. 2B, E). The lower one-fourth of the height of the lateral surface of the dentary is perforated by four anteroposteriorly elongated, ovoid foramina that pierce the floor of the inferior alveolar canal (Figs. 2B, E, G, 3A, B, D, I). These foramina are arranged parallel to the ventral margin of the dentary and positioned between the level of the second and seventh preserved dentary teeth. They are evenly spaced from one another, separated by a gap not much greater than the diameter of each foramen. Above this row of foramina, a pair of sinuous, parallel grooves and ridges are present on the middle one-third of the lateral surface of the dentary (Fig. 2B, E–G). The grooves are deepest anteriorly, shallowest posteriorly, and oriented slightly posteroventrally. The dorsolateral surface of the dentary below the teeth and above the dorsal-most lateral groove is mostly smooth. There is no prominent layer or lip of secondary bone on the lateral surface of the jaw, which may indicate that GSI/SR/PAL-NR-0101 is from an immature individual (see Discussion).

Maxillary tooth wear facets are carved into the dorsolateral surface of the dentary adjacent to the first four teeth (Figs. 2E–G, 3A, C). The most prominent facet is oriented vertically and extends upward onto the mesiolabial surface of the base of the fourth tooth. This facet is continuous with the shallower one adjacent to the larger third tooth. A pair of faint, vertically oblique ridges of unworn/less worn bone occurs lateral to the first and second teeth. These ridges separate the shallow wear facets between the first three teeth and the one that is broken off mesial to the first preserved tooth. When combined, these four facets form a nearly continuous, weakly undulate, and anteroposteriorly elongate wear facet with an outer margin that is weakly convex posteriorly and nearly straight ventrally. Poor separation of the individual wear facets suggests a low degree of proal jaw motion (i.e., a forward stroke of the dentary after jaw closure; see Jones et al., 2012), but the major motion was likely orthal (scissor-like). The height of this wear surface is shorter anteriorly and slightly taller posteriorly and extends downward for about the upper one fourth of the height of the dentary. As discussed below, the deep scour marks on the dentary adjacent to the antepenultimate and penultimate teeth are most likely not maxillary tooth wear facets.

Dentary Teeth

Nine teeth are preserved in GSI/SR/PAL-NR-0101. The second and fourth teeth are the best preserved, but most show some level of pre- and/or postmortem breakage, wear, or corrosion (e.g., Fig. 3E–G). Thus, aspects of the teeth that are often important in diagnosing rhynchocephalian taxa cannot fully be documented here (e.g., flange size and shape), limiting our ability to make more reliable inferences about the lower-level taxonomic affinities of GSI/SR/PAL-NR-0101.

The teeth are acrodont in their mode of attachment, ankylosed to the crest of the dentary. The three smallest teeth are set more shallowly onto the bone. There is no thickened layer of secondary bone covering the bases of the teeth (Fig. 3E–G), and our μCT scan slices reveal no distinct density differences between the tooth enamel, dentine, and adjacent dentary bone (Fig. 3B, C). Three-dimensional modeling of the jaw and teeth reveals that most teeth have a central pulp cavity that is connected to the inferior alveolar canal via a single, narrow vascular canal in smaller teeth, or a network of vascular canals in larger teeth (Fig. 3B–D).

The nine teeth include at least six mesial teeth that alternate in size and represent the hatchling series, at least two poorly preserved distal teeth that likely represent the anterior additionals, and a partial tooth positioned between them that either represents the last hatchling tooth or the first additional (Fig. 3E). No successional teeth are observed. The smaller hatchling teeth are placed in line with the labial half of the larger hatchling teeth (labeled "h" and "H," respectively in Fig. 3E). The teeth are not crowded along the tooth row, but in some cases, they nearly abut or weakly overlap each other at their bases.

The larger hatchling teeth are variably broken mesially, distally, and apically; the distal most small hatchling tooth (h6) also is broken apically (Fig. 3E). This damage has formed sharp edges that, in some cases falsely resemble flanges and crests (e.g., "H3" in Fig. 3E, F). Regions of the enamel on these larger teeth are variably pitted and unevenly eroded down to the dentine layer, which is most prominent lingually on H3 (Fig. 3F) and labially on H5 (Fig. 3G). Where the enamel is preserved, the surface is smooth and without vertical striae. Despite the level of damage to each of the larger hatchling teeth, we interpret them as having been scaled-up versions of the smaller hatchling teeth (i.e., h2 and h4).

The hatchling teeth, as exemplified by h2 and h4, are labiolingually compressed, mesially tipped cones with weak crests and carinae. The lingual or labial profile of the triangular crown of h2 and h4 is slightly concavoconvex (i.e., mesially concave and distally convex, respectively), and their mesial margins are more vertically oriented, whereas their distal margins are oriented more obliquely. Consequently, the crown apex is offset to the mesial side of the tooth. The distal margins of h2 and h4 have a distinct break in slope below the triangular crown, which is nearly vertical in orientation and slightly concave in contour. The mesiolabial edge of h2 and h4 forms a labiolingually thin crest (Fig. 3E), and the mesiolingual surface of the crown is indented with a shallow vertical depression (Fig. 2D). The relatively larger first hatchling tooth (H1) has a similarly narrow mesiolabial crest, but the surface lingual to it is only weakly concave. The distal half of both h2 and h4 possesses a weak distolabial carina that extends basalward from the crown apex to the base of the triangular crown and where the break in slope begins (Fig. 3E).

The lingual and labial crown faces of h2 and h4 are convex in horizontal section (Fig. 2C). Each tooth tapers toward the mesial and, to a lesser extent, distal edge. The cross-section of tooth h6 is rounded. Relative to h2 and h4, the mesiolabial crest in h6 is reduced to a carina but retains the distolabial carina. In occlusal view, h2, h4, and h6 are set at a slightly oblique angle (more so in h6) to the long axis of the tooth row such that the mesiolabial crest/carina is positioned more labially than is the distolabial carina. The basal cross-section of each of the larger hatchling teeth (H1, H3, H5) and H/A is ovoid in marginal outline and longer mesiodistally than wide labiolingually. The mesiodistal length of each of the smaller hatchling teeth is between about two-thirds to one-half that of these larger teeth; each of the smaller teeth is up to nearly three-fourths the labiolingual width of the larger ones. In general, the basal length and width of the hatchling teeth increase distally along the tooth row, and we suspect crown height similarly increased.

The lingual face of H5 (and perhaps H3) has a pair of dull, vertical ridges, one each on the mesiolingual and distolingual edges of the tooth (Figs. 2C, D, 3E). Consequently, this tooth is more pyramidal in form relative to the other hatchling teeth, which are essentially mesially leaning, labiolingually compressed cones. Most of the labial surface of H5 is eroded, uneven, and not polished by attritional wear (Figs. 2B, 3G), and the mesiolabial and distolabial margins are worn away toward the apex (Fig. 3E). This wear has obscured the true marginal outline of this tooth, which appears symmetrical as preserved but more likely was asymmetrical as observed in the better-preserved hatchling teeth. The deeply incised and vertically oblique scour mark on the labial side of H/A and the dentary at that level reveals the internal layers of and contact between the tooth and bone (Figs. 2B, C, E–G, 3A, H). Here, the cracks in the tooth dentine are vertically oriented, whereas the cracks in the dentary are horizontally oriented. H/A is ventrally convex along its basal contact with the dentary (Fig. 3H). Ventral to and in line with the scour mark that is adjacent to H/A is a similar looking mark that is positioned behind the fourth foramen on the ventrolateral side of the dentary and is oriented at an oblique angle anterodorsally/posteroventrally (Figs. 2B, E, G, 3A, I). This ventrolateral scour mark also reveals horizontal cracks in the dentary bone. Both the ventrolateral scour mark and the one carved into and adjacent H/A appear to have originated from the same or similar mechanical source, given their similar size, shape, depth, and lateral position anteroposteriorly. Because the ventrolateral scour mark cannot be the result of attritional wear from the Naskal rhynchocephalian's own maxillary teeth, it follows that the one adjacent H/A likely is not a maxillary tooth wear facet either.

The two additional teeth (A1, A2) are poorly preserved (Figs. 2, 3E). Only the base of A1 and a little of the enamel from its distal surface are preserved. In occlusal view, the base of this

tooth is similar in size to the base of H/A (Fig. 2C). On its distolabial side and down onto the dorsolateral surface of the dentary is a relatively shallow, vertically oblique mark with an uneven surface (Figs. 2B, E, F, 3A, H). This mark does not appear to be a maxillary tooth wear facet given its unpolished surface (e.g., compare with the polished wear facet adjacent H1–h4 in Figs. 2E–G, 3A). The surface may have been chipped during collection or screenwashing. The second additional tooth (A2) preserves the lower half of the crown, but its distal portion is broken off. As a result, the pulp cavity is exposed (e.g., Fig. 3D). The enamel surface is smooth on the labial, mesiolingual, and upper lingual surfaces of the tooth. Most of the lingual side of this tooth is pitted, and its surface is flattened (Figs. 2C, D, 3E). No natural flanges are apparent.

COMPARATIVE ANATOMY

The Naskal rhynchocephalian (GSI/SR/PAL-NR-0101) is a member of Acrosphenodontia based on its regionalized, acrodont marginal dentition (e.g., Chambi-Trowell et al., 2021; DeMar et al., in press). It is difficult to determine its lower-level taxonomic affinities because there are few preserved features for comparison. Additionally, GSI/SR/PAL-NR-0101 appears to be from an immature individual, based on its small size, the minor attritional wear of its teeth, and the thin or absent secondary bone on the dentary and around the bases of its teeth (Robinson, 1976; Fraser, 1988). Furthermore, because the hatchling series typically wears down with age and, in some cases, is completely lost in mature individuals (e.g., Robinson, 1976; Fraser, 1988; Simões et al., 2022), comparisons of these teeth are mostly restricted to immature individuals. Lastly, relative to the successional and additional teeth in most rhynchocephalians, the hatchling teeth are simple structures (e.g., labiolingually compressed cones that alternate in size) and provide few distinguishing characters for comparative anatomy and taxonomy. Despite these complicating factors, we make comparisons of GSI/SR/PAL-NR-0101 with the few other acrosphenodontians that have reasonably well-preserved hatchling teeth (as described and figured in the literature and based on the original high-resolution images of *Rebbanosaurus jaini* and *Godavarisaurus lateefi* in Evans et al., 2001).

The alternating-sized hatchling teeth in GSI/SR/PAL-NR-0101 are distinct from all other acrosphenodontians in possessing the following combination of features (as observed in some or all these teeth): teeth not crowded; enamel smooth; teeth labiolingually compressed in occlusal view, with ovoid, teardrop-shaped, or rounded bases; distinct break in slope along distal margin (i.e., oblique orientation to nearly vertical); labial profile of crown concave mesially and convex distally (i.e., concavoconvex); crown apex offset mesially; mesiolabial crest and weak distolabial carina present; and crown mesiolingual surface vertically indented with shallow depression. The Naskal taxon clearly differs from the basally branching acrosphenodontian *Planocephalosaurus robinsonae* from the Upper Triassic of the U.K. (Fraser, 1982; Herrera-Flores et al., 2018) and the Early Cretaceous *Pamizinsaurus tlayuaensis* of Mexico (Reynoso, 1997) in lacking vertically striated hatchling teeth. The Naskal taxon also differs from the following acrosphenodontians in lacking simple, cone-shaped hatchling teeth with a centered (or at least not mesially offset) crown apex: *Lanceirosphenodon ferigoloi* (Late Triassic, Brazil; Romo de Vivar et al., 2020); *Cynosphenodon huizachalensis* (Early Jurassic, Mexico; Reynoso, 1996, 2003); *Clevosaurus convalis* (Early Jurassic, UK; Säilä, 2005); *Sphenocondor gracilis* (Middle Jurassic, Patagonia, Argentina; Apesteguía and Jones 2012); *Tingitana anoualae* (Early Cretaceous, Morocco; Evans and Sigogneau-Russell, 1997); and *Sphenodon punctatus* (Robinson, 1976). The hatchling teeth in juvenile *Clevosaurus hudsoni* (Late Triassic, UK) bear a distinct mesial and distal flange (Fraser, 1988), which are lacking in the Naskal taxon.

The Naskal taxon differs from *Rebbanosaurus jaini* and *Godavarisaurus lateefi* (Evans et al., 2001), both collected from the Lower–Middle Jurassic Kota Formation about 300 km northeast of Naskal (Fig. 1A). The Naskal taxon differs from *R. jaini* in having a subdental shelf that decreases in height posteriorly (vs. being tall along its full length) and a Meckelian groove that deepens dorsoventrally posteriorly (vs. staying the same height and being limited to the ventral border of the dentary). Few complete hatchling teeth are preserved in *R. jaini*, limiting further comparisons.

The Naskal taxon differs from the juvenile dentary of *Godavarisaurus lateefi* (VPL/JU/KR39; Evans et al., 2001:fig. 14E, F) in lacking a diastema between the hatchling and additional teeth but resembles it in the decreasing height of the subdental shelf and the deepening of the Meckelian groove. It is unknown whether a diastema is a juvenile feature in *G. lateefi*, because the region between the hatchling and additional teeth is not preserved in any of the five larger, more mature dentaries currently known (see Evans et al., 2001). Therefore, the absence of the diastema in the Naskal taxon is only a tentative difference between it and *G. lateefi*.

The small hatchling teeth of the Naskal taxon (i.e., h2, h4, and h6) differ from the two small mesial ones in *Godavarisaurus lateefi* (VPL/JU/KR39, 'h2' and 'h4') in having a distinct break in slope along the distal margin, a concavoconvex crown profile, a mesially offset crown apex, and a distinct but shallow vertical depression on the mesiolingual surface of the crown. The distal-most small hatchling tooth in *G. lateefi* (VPL/JU/KR39, 'h6') most closely resembles those in the Naskal taxon in having a mesially offset crown apex and a distinct break in slope along its distal margin (assuming the tooth crown and posteriorly adjacent portion of the jawbone are not broken in VPL/JU/KR39). Comparisons with the larger hatchling teeth are more difficult to make due to the broken crowns in GSI/SR/PAL-NR-0101 (Fig. 3E–H), but the shared presence of a weak mesiolingual and distolingual vertical ridge can be seen on the fifth preserved tooth from the anterior (H5 and 'H5') in both the Naskal taxon (GSI/SR/PAL-NR-0101) and *G. lateefi* (VPL/JU/KR39); a distinct distolingual ridge is also present on 'H3' in VPL/JU/KR39. Both 'H3' and 'H5' in *G. lateefi* (VPL/JU/KR39) also have concavoconvex profiles, but only in the latter tooth is its crown apex mesially offset. The Naskal taxon (GSI/SR/PAL-NR-0101) and *G. lateefi* (VPL/JU/KR39) also have a lingually flattened additional tooth (Figs. 2C, D, 3E vs. Evans et al., 2001:fig. 14F). Overall, the Naskal taxon appears to be more similar in morphology to *G. lateefi* than to any other acrosphenodontian.

DISCUSSION AND CONCLUSIONS

The discovery of GSI/SR/PAL-NR-0101 indicates that the record of Rhynchocephalia in India spans most of the Mesozoic, from the early Late Triassic (Carnian) to the latest Cretaceous or earliest Paleocene (< 100 kyr interval spanning the K–Pg boundary). This temporal range is surpassed only by the record in Argentina, which extends from slightly earlier in the Carnian to the Paleocene (Apesteguía et al., 2014; Hsiou et al., 2019).

The broad temporal separation of the three horizons preserving rhynchocephalians in India (Tiki and Kota formations, Naskal intertrappean) and the fragmentary nature of the specimens collected to date make it extremely difficult to track their evolution on the subcontinent, but coarse taxonomic assessments are possible. The Tiki Formation maxilla (Ray et al., 2016:fig. 7F–H) and Naskal dentary have uncertain phylogenetic relationships with *Rebbanosaurus jaini* and *Godavarisaurus lateefi*, whose phylogenetic positions are currently in a state of flux (e.g., see

cladograms in Romo de Vivar et al., 2020; Chambi-Trowell et al., 2021; DeMar et al., in press). Nevertheless, one feature that might link the Tiki Formation rhynchocephalian to *Rebbanosaurus jaini* is the shared presence of radially arranged, apicobasally striated, acrodont additional maxillary teeth, which is not known in the Naskal taxon nor present in *Godavarisaurus* (Ray et al., 2016:fig. 7F–H vs. Evans et al., 2001:fig. 3K). However, this combination of features is also present in taxa from outside India (e.g., *Planocephalosaurus robinsonae*: Fraser, 1982; *Pamizinsaurus tlayuaensis*: Reynoso, 1997; *Micromenodon pitti*: Sues and Schoch, 2021). Likewise, the Naskal taxon might be closely related to *Godavarisaurus lateefi* as discussed above, but more complete material is needed to test this hypothesis.

Discovery of the Naskal rhynchocephalian reinforces the emerging pattern that the group was confined to the southern landmasses of Gondwana after the Early Cretaceous (Evans et al., 2001; Apesteguía and Novas, 2003; Martinelli and Forasiepi, 2004; Apesteguía, 2005; Apesteguía and Rougier, 2007; Apesteguía and Jones, 2012; Apesteguía et al., 2014, 2021; Apesteguía and Carballido, 2014; Gentil et al., 2019; Fig. 4). All but the Naskal taxon are from South America and considered members of the deeply nested clades Sphenodontinae and Opisthodontia or Eilenodontinae (e.g., Apesteguía et al., 2014, 2021; Gentil et al., 2019; Chambi-Trowell et al., 2021). The possible relationship between the Naskal taxon and *Godavarisaurus* would suggest that the Naskal taxon is phylogenetically near the base of Acrosphenodontia, well outside the clades that contain the Late Cretaceous South American forms (e.g., Romo de Vivar et al., 2020; Chambi-Trowell et al., 2021; DeMar et al., in press). Thus, the Naskal taxon might represent a late-surviving relic species.

Little is known about the effects of the end-Cretaceous mass extinction on rhynchocephalian diversity. Non-marine squamates in the Western Interior of North America suffered high species extinctions (81–83%) across the K–Pg boundary (Longrich et al., 2012; DeMar, 2016), whereas only two rhynchocephalian lineages are known to have survived the extinction event (Apesteguía et al., 2014). The survivors include the genus *Kawasphenodon* from Patagonia (Apesteguía, 2005; Apesteguía et al., 2014) and the lineage that ultimately gave rise to *Sphenodon punctatus*. The Naskal taxon might represent a third surviving lineage, which not only would represent higher species-level survivorship, but also higher clade-level survivorship given its possible relationship to *Godavarisaurus*. Ultimately, the validity of this hypothesis depends on the true age of the Naskal locality, which is currently considered most likely uppermost Cretaceous but possibly lowermost Paleocene (< 100 kyr spanning the K–Pg boundary; Wilson Mantilla et al., 2022), and continued sampling of Paleogene horizons in India (e.g., Bajpai and Thewissen, 2002; Rana et al., 2005; Bajpai et al., 2009; Rose et al., 2019; Kapur et al., 2022).

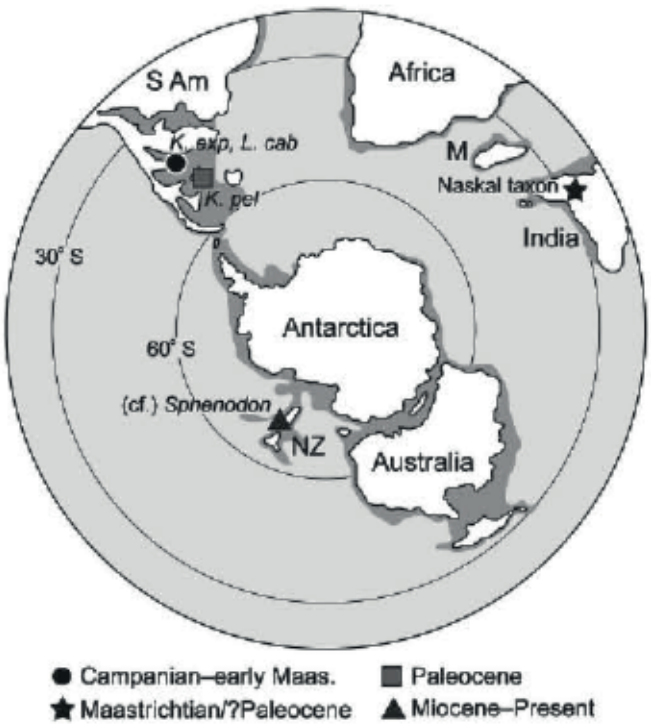

FIGURE 4. Map of the southern hemisphere during the latest Cretaceous (Maastrichtian, ~66 Ma) showing the paleobiogeographic distributions of unambiguous Rhynchocephalia from the Campanian to Present (map redrawn and modified from Apesteguía et al., 2014). Fossil records for each taxon are: *Kawasphenodon* (Apesteguía 2005; Apesteguía et al. 2014), *Lamarquesaurus cabazai* (Apesteguía and Rougier, 2007), (cf.) *Sphenodon* (= cf. *Sphenodon* sp. and *S. punctatus*) (Jones et al., 2009), and the Naskal taxon (this study). Continental shelves are shaded medium gray. **Abbreviations**: ***K. exp***, *Kawasphenodon expectatus*; ***K. pel***, *Kawasphenodon peligrensis*; ***L. cab***, *Lamarquesaurus cabazai*; **M**, Madagascar; **Maas.**, Maastrichtian; **NZ**, New Zealand; **S Am**, South America.

ACKNOWLEDGMENTS

SA thanks GSI and Presidency College for providing access to fossil samples and laboratory research facilities. We thank S. Santana for access to the Santana Lab µCT scanner, B. Hovatter for µCT scanning, H. Fulghum for preliminary µCT data processing and 3D renderings, and M. Holland for reproduction of 3D print casts. We thank S. Evans for providing us with the high-resolution images of *Rebbanosaurus jaini* and *Godavarisaurus lateefi* for comparison. We thank M.E.H. Jones for comments on an earlier version of this manuscript. S. Evans and P. Romo de Vivar Martínez provided constructive reviews of this manuscript, and Associate Editor E. Maxwell and the technical editors provided useful suggestions. This research was supported by a grant from the National Science Foundation to co-PIs GPWM (EAR-1736787) and JAWM (EAR-1736606), grants from UCMP Welles Fund, the National Geographic Society, and the UW Royalty Research Fund to GPWM.

ORCID

S. Anantharaman http://orcid.org/0000-0001-8432-3605
David G. DeMar Jr. http://orcid.org/0000-0001-5426-0471
Gregory P. Wilson Mantilla http://orcid.org/0000-0003-3604-5473
Jeffrey A. Wilson Mantilla http://orcid.org/0000-0003-2469-7028

LITERATURE CITED

Anantharaman, S., and D. C. Das Sarma. 1997. Palaeontological studies on the search of micromammals in the infra and intertrappean sediments of Karnatak. Records of the Geological Survey of India 130:239–240.

Apesteguía, S. 2005. A Late Campanian sphenodontid (Reptilia, Diapsida) from northern Patagonia. Comptes Rendus Palevol 4:663–669.

Apesteguía, S., and J. L. Carballido. 2014. A new eilenodontine (Lepidosauria, Sphenodontidae) from the Lower Cretaceous of central Patagonia. Journal of Vertebrate Paleontology 34:303–317.

Apesteguía, S., and M. E. H. Jones. 2012. A Late Cretaceous "tuatara" (Lepidosauria: Sphenodontinae) from South America. Cretaceous Research 34:154–160.

Apesteguía, S., and F. E. Novas. 2003. Large Cretaceous sphenodontian from Patagonia provides insight into lepidosaur evolution in Gondwana. Nature 425:609–612.

Apesteguía, S., and G. W. Rougier. 2007. A Late Campanian sphenodontid maxilla from northern Patagonia. American Museum Novitates 3581:1–11.

Apesteguía, S., F. F. Garberoglio, and R. O. Gómez. 2021. Earliest tuatara relative (Lepidosauria: Sphenodontinae) from southern continents. Ameghiniana 58:416–441.

Apesteguía, S., R. O. Gómez, and G. W. Rougier. 2012. A basal sphenodontian (Lepidosauria) from the Jurassic of Patagonia: new insights on the phylogeny and biogeography of Gondwanan rhynchocephalians. Zoological Journal of the Linnean Society 166:342–360.

Apesteguía, S., R. O. Gómez, and G. W. Rougier. 2014. The youngest South American rhynchocephalian, a survivor of the K/Pg extinction. Proceedings of the Royal Society B 281:1–6.

Augé, M., and J.-C. Rage. 2006. Herpetofaunas from the Upper Paleocene and Lower Eocene of Morocco. Annales de Paléontologie 92:235–253.

Bajpai, S., and J. G. M. Thewissen. 2002. Vertebrate fauna from Panandhro lignite field (lower Eocene), District Kachchh, western India. Current Science 82:507–509.

Bajpai, S., V. V. Kapur, and J. G. M. Thewissen. 2009. Creodont and condylarth from the Cambay Shale (early Eocene, ~55–54 Ma), Vastan Lignite Mine, Gujarat, western India. Journal of the Palaeontological Society of India 54:103–109.

Carroll, R. L. 1985. A pleurosaur from the Lower Jurassic and the taxonomic position of the Sphenodontida. Palaeontographica Abteilung A 189:1–28.

Cau, A., M. A. Baiano, and P. Raia. 2014. A new sphenodontian (Reptilia, Lepidosauria) from the Lower Cretaceous of Southern Italy and the phylogenetic affinities of the Pietraroia Plattenkalk rhynchocephalians. Cretaceous Research 49:172–180.

Chambi-Trowell, S. A. V., A. G. Martinelli, D. I. Whiteside, P. R. Romo de Vivar, M. B. Soares, C. L. Schultz, P. G. Gill, M. J. Benton, and E. J. Rayfield. 2021. The diversity of Triassic South American sphenodontians: a new basal form, clevosaurs, and a revision of rhynchocephalian phylogeny. Journal of Systematic Palaeontology 19:787–820.

Conrad, J. L. 2018. A new lizard (Squamata) was the last meal of *Compsognathus* (Theropoda: Dinosauria) and is a holotype in a holotype. Zoological Journal of the Linnean Society 183:584–634.

Cree, A. 2014. Tuatara: biology and conservation of a venerable survivor. Canterbury University Press, Christchurch, New Zealand, 583 pp.

Das Sarma, D. C., S. Anantharaman, G. Vijayasarathi, T. T. Nath, and C. V. Rao. 1995. Palaeontological studies for the search of micromammals in the infra- and intertrappean horizons of Andhra Pradesh. Records of the Geological Survey of India 128:223.

Datta, P. M., D. P. Das, and Z.-X. Luo. 2004. A Late Triassic dromatheriid (Synapsida: Cynodontia) from India. Annals of Carnegie Museum 73:12–24.

DeMar, D. G., Jr. 2016. Late Cretaceous and Paleocene Lissamphibia and Squamata of Montana and the end-Cretaceous mass extinction. Ph.D. dissertation, University of Washington, Seattle, Washington, 334 pp.

DeMar, D. G., Jr., M. E. H. Jones, and M. T. Carrano. In press. A nearly complete skeleton of a new eusphenodontian from the Upper Jurassic Morrison Formation, Wyoming, USA provides insight into the evolution and diversity of Rhynchocephalia (Reptilia: Lepidosauria). Journal of Systematic Palaeontology.

de Queiroz, K., and J. A. Gauthier. 2020. Lepidosauria; pp. 1079–1085 in K. de Queiroz, P. D. Cantino, and J. A. Gauthier (eds.), Phylonyms: A Companion to the PhyloCode. CRC Press, Boca Raton.

Dutt, N. V. B. S. 1975. Deccan traps of the western part of Hyderabad District, Andhra Pradesh. Records of the Geological Survey of India 106:114–126.

Evans, S. E. 1980. The skull of a new eosuchian reptile from the Lower Jurassic of South Wales. Zoological Journal of the Linnean Society 70:203–264.

Evans, S. E. 1981. The postcranial skeleton of the Lower Jurassic eosuchian *Gephyrosaurus bridensis*. Zoological Journal of the Linnean Society 73:81–116.

Evans, S. E. 1984. The classification of the Lepidosauria. Zoological Journal of the Linnean Society 82:87–100.

Evans, S.E. 1995. Lizards: evolution, early radiation and biogeography; pp. 271–283 in A. Sun and Y. Wang (eds.), Sixth Symposium on Mesozoic Terrestrial Ecosystems and Biota, Short Papers. China Ocean Press, Beijing.

Evans, S. E. 1998. Lepidosaurian faunas from the Early Cretaceous: a clade in transition. New Mexico Museum of Natural History and Science Bulletin 14:195–200.

Evans, S. E., and M. Borsuk-Białynicka. 2009. A small lepidosauromorph reptile from the Early Triassic of Poland. Palaeontologia Polonica 65:179–202.

Evans, S. E., and D. Sigogneau-Russell. 1997. New sphenodontians (Diapsida: Lepidosauria: Rhynchocephalia) from the Early Cretaceous of North Africa. Journal of Vertebrate Paleontology 17:45–51.

Evans, S. E., G. V. R. Prasad, and B. K. Manhas. 2001. Rhynchocephalians (Diapsida: Lepidosauria) from the Jurassic Kota Formation of India. Zoological Journal of the Linnean Society 133:309–334.

Evans, S. E., G. V. R. Prasad, and B. K. Manhas. 2002. Fossil lizards from the Jurassic Kota Formation of India. Journal of Vertebrate Paleontology 22:299–312.

Fraser, N. C. 1982. A new rhynchocephalian from the British Upper Trias. Palaeontology 25:709–725.

Fraser, N. C. 1988. The osteology and relationships of *Clevosaurus* (Reptilia: Sphenodontida). Philosophical Transactions of the Royal Society of London B 321:125–178.

Gauthier, J. A., R. Estes, and K. de Queiroz. 1988. A phylogenetic analysis of Lepidosauromorpha; pp. 15–98 in R. Estes and G. Pregill (eds.) Phylogenetic Relationships of the Lizard Families. Stanford University Press, Stanford, California.

Gentil, A. R., F. L. Agnolin, J. A. Garcia Marsà, M. J. Motta, and F. E. Novas. 2019. Bridging the gap: sphenodont remains from the Turonian (Upper Cretaceous) of Patagonia. Palaeobiological inferences. Cretaceous Research 98:72–83.

Günther, A. 1867. Contribution to the anatomy of *Hatteria* (*Rhynchocephalus*, Owen). Philosophical Transactions of the Royal Society of London 157:595–629.

Haeckel, E. 1866. Generelle Morphologie der Organismen. II: Allgemeine Entwicklungsgeschichte der Organismen. Verlag Georg Reimer, Berlin, 574 pp.

Herrera-Flores, J. A., T. L. Stubbs, and M. J. Benton. 2021. Ecomorphological diversification of squamates in the Cretaceous. Royal Society Open Science 8:201961.

Herrera-Flores, J. A., T. L. Stubbs, A. Elsler, and M. J. Benton. 2018. Taxonomic reassessment of *Clevosaurus latidens* Fraser, 1993 (Lepidosauria, Rhynchocephalia) and rhynchocephalian phylogeny based on parsimony and Bayesian inference. Journal of Paleontology 92:734–742.

Hsiou, A. S., R. L. Nydam, T. R. Simões, F. A. Pretto, S. Onary, A. G. Martinelli, A. Liparini, P. R. R. de V. Martínez, M. B. Soares, C. L. Schultz, and M. W. Caldwell. 2019. A new clevosaurid from the Triassic (Carnian) of Brazil and the rise of sphenodontians in Gondwana. Scientific Reports 9:11821.

Jitendra, K. and K. Sh. Milankumar. 2019. Micro and mega-vertebrate fossils from the Late Triassic Tiki Formation, South Rewa Gondwana Basin, India: palaeoenvironmental and palaeobiogeographic implications. Journal of the Palaeontological Society of India 64:151–168.

Jones, M. E. H. 2006a. The Early Jurassic clevosaurs from China (Diapsida: Lepidosauria). New Mexico Museum of Natural History and Science Bulletin 37:548–562.

Jones, M. E. H. 2006b. Tooth diversity and function in the Rhynchocephalia (Diapsida: Lepidosauria); pp. 55–58 in P. M. Barrett and S. E. Evans (eds.), Ninth international symposium on Mesozoic terrestrial ecosystems and biota. Natural History Museum, London, UK.

Jones, M. E. H. 2008. Skull shape and feeding strategy in *Sphenodon* and other Rhynchocephalia (Diapsida: Lepidosauria). Journal of Morphology 269:945–966.

Jones, M. E. H. 2009. Dentary tooth shape in *Sphenodon* and its fossil relatives (Diapsida: Lepidosauria: Rhynchocephalia); pp. 9–15 in T. Koppe, G. Meyer, and K. W. Alt (eds.), Interdisciplinary Dental Morphology, Frontiers of Oral Biology (vol. 13). Karger, Greifswald, Germany.

Jones, M. E. H., P. O'Higgins, M. J. Fagan, S. E. Evans, and N. Curtis. 2012. Shearing mechanics and the influence of a flexible symphysis during oral food processing in *Sphenodon* (Lepidosauria: Rhynchocephalia). The Anatomical Record: Advances in Integrative Anatomy and Evolutionary Biology 295:1075–1091.

Jones, M. E. H., A. J. D. Tennyson, J. P. Worthy, S. E. Evans, and T. H. Worthy. 2009. A sphenodontine (Rhynchocephalia) from the

Miocene of New Zealand and palaeobiogeography of the tuatara (*Sphenodon*). Proceedings of the Royal Society B 276:1385–1390.

Jones, M. E. H., C. Anderson, C. A. Hipsley, J. Müller, S. E. Evans, and R. R. Schoch. 2013. Integration of molecules and new fossils supports a Triassic origin for Lepidosauria (lizards, snakes, and tuatara). BMC Evolutionary Biology 13:208.

Kapur, V. V., N. Carolin, and S. Bajpai. 2022. Early Paleogene mammal faunas of India: a review of recent advances with implications for the timing of initial India-Asia contact. Himalayan Geology 43:337–356.

Khajuria, C. K., and G. V. R. Prasad. 1998. Taphonomy of a Late Cretaceous mammal-bearing microvertebrate assemblage from the Deccan inter-trappean beds of Naskal, peninsular India. Palaeogeography, Palaeoclimatology, Palaeoecology 137:153–172.

LeBlanc, A. R. H., S. Apesteguía, H. C. E. Larsson, and M. W. Caldwell. 2020. Unique tooth morphology and prismatic enamel in Late Cretaceous sphenodontians from Argentina. Current Biology 30:1755–1761.

Longrich, N. R., B. A. S. Bhullar, and J. A. Gauthier. 2012. Mass extinction of lizards and snakes at the Cretaceous–Paleogene boundary. Proceedings of the National Academy of Sciences 109:21396–21401.

Martinelli, A. G., and A. M. Forasiepi. 2004. Late Cretaceous vertebrates from Bajo de Santa Rosa (Allen Formation), Río Negro Province, Argentina, with the description of a new sauropod dinosaur (Titanosauridae). Revista del Museo Argentino de Ciencias Naturales 6:257–305.

Prasad, G. V. R. 2012. Vertebrate biodiversity of the Deccan volcanic province of India: a review. Bulletin de la Société géologique de France 183:597–610.

Prasad, G. V. R., and A. Sahni. 1988. First Cretaceous mammal from India. Nature 332:638–640.

Prasad, G. V. R., J. J. Jaeger, A. Sahni, E. Gheerbrant, and C. K. Khajuria. 1994. Eutherian mammals from the Upper Cretaceous (Maastrichtian) intertrappean beds of Naskal, Andhra Pradesh, India. Journal of Vertebrate Paleontology 14:260–277.

Rana, R. S., K. Kumar, H. Singh, and K. D. Rose. 2005. Lower vertebrates from the Late Palaeocene–Earliest Eocene Akli Formation, Giral Lignite Mine, Barmer District, western India. Current Science 89:1606–1613.

Rauhut, O. W. M., A. M. Heyng, A. López-Arbarello, A. Hecker. 2012. A new rhynchocephalian from the Late Jurassic of Germany with a dentition that is unique amongst tetrapods. PLoS ONE 7:e46839.

Ray, S., M. S. Bhat, D. Mukherjee, and P. M. Datta. 2016. Vertebrate fauna from the Late Triassic Tiki Formation of India: new finds and their biostratigraphic implications. The Palaeobotanist 65:47–59.

Reynoso, V.-H. 1996. A Middle Jurassic *Sphenodon*-like sphenodontian (Diapsida:Lepidosauria) from Huizachal Canyon, Tamaulipas, México. Journal of Vertebrate Paleontology 16:210–221.

Reynoso, V.-H. 1997. A "beaded" sphenodontian (Diapsida: Lepidosauria) from the Early Cretaceous of central Mexico. Journal of Vertebrate Paleontology 17:52–59.

Reynoso, V.-H. 2000. An unusual aquatic sphenodontian (Reptilia: Diapsida) from the Tlayua Formation (Albian), Central Mexico. Journal of Paleontology 74:133–148.

Reynoso, V.-H. 2003. Growth patterns and ontogenetic variation of the teeth and jaws of the Middle Jurassic sphenodontian *Cynosphenodon huizachalensis* (Reptilia: Rhynchocephalia). Canadian Journal of Earth Sciences 40:609–619.

Robinson, P. L. 1976. How *Sphenodon* and *Uromastyx* grow their teeth and use them; pp. 43–65 in A. d'A. Bellairs and C. B. Cox (eds.), Morphology and Biology of Reptiles. Academic Press Inc., London, Linnean Society Symposium Series, 3.

Romo de Vivar, P. R., A. G. Martinelli, A. S. Hsiou, and M. B. Soares. 2020. A new rhynchocephalian from the Late Triassic of southern Brazil enhances eusphenodontian diversity. Journal of Systematic Palaeontology 18:1103–1126.

Rose, K. D., L. T. Holbrook, K. Kumar, R. S. Rana, H. E. Ahrens, R. H. Dunn, A. Folie, K. E. Jones, and T. Smith. 2019. Anatomy, relationships, and paleobiology of *Cambaytherium* (Mammalia, Perissodactylamorpha, Anthracobunia) from the lower Eocene of western India. Society of Vertebrate Paleontology Memoir 20. Journal of Vertebrate Paleontology 39(6, Supplement):1–147.

Säilä, L. K. 2005. A new species of the sphenodontian reptile *Clevosaurus* from the Lower Jurassic of South Wales. Palaeontology 48:817–831.

Simões, T. R., M. W. Caldwell, and S. E. Pierce. 2020. Sphenodontian phylogeny and the impact of model choice in Bayesian morphological clock estimates of divergence times and evolutionary rates. BMC Biology 18:191.

Simões, T. R., G. Kinney-Broderick, and S. E. Pierce. 2022. An exceptionally preserved *Sphenodon*-like sphenodontian reveals deep time conservation of the tuatara skeleton and ontogeny. Communications Biology 5:195.

Smith, K. T., O. Comay, L. Maul, F. Wegmüller, J.-M. Le Tensorer, and T. Dayan. 2021. A model of digestive tooth corrosion in lizards: experimental tests and taphonomic implications. Scientific Reports 11:12877.

Sues, H.-D., and R. R. Schoch. 2021. A new early-diverging sphenodontian (Lepidosauria, Rhynchocephalia) from the Upper Triassic of Virginia, U.S.A. Journal of Paleontology 95:344–350.

Throckmorton, G. S., J. A. Hopson, and P. Parks. 1981. A redescription of *Toxolophosaurus cloudi* Olson, a Lower Cretaceous herbivorous sphenodontid reptile. Journal of Paleontology 55:586–597.

Uetz, P., P. Freed, R. Aguilar, and J. Hošek (eds). 2022. The Reptile Database. Available at www.reptile-database.org. Accessed March 21, 2022.

Whiteside, D. I. 1986. The head skeleton of the Rhaetian sphenodontid *Diphydontosaurus avonis* gen. et sp. nov. and the modernizing of a living fossil. Philosophical Transactions of the Royal Society of London Series B 312:379–430.

Williston, S. W. 1925. The Osteology of the Reptiles. Harvard University Press, Cambridge, 300 pp.

Wilson, G. P., D. C. Das Sarma, and S. Anantharaman. 2007. Late Cretaceous sudamericid gondwanatherians from India with paleobiogeographic consideration of Gondwanan mammals. Journal of Vertebrate Paleontology 27:521–531.

Wilson, J. A., D. M. Mohabey, P. Lakra, and A. Bhadran. 2019. Titanosaur (Dinosauria: Sauropoda) vertebrae from the Upper Cretaceous Lameta Formation of western and central India. Contributions from the Museum of Paleontology, University of Michigan 33:1–27.

Wilson Mantilla, G. P., P. R. Renne, B. Samant, D. M. Mohabey, A. Dhobale, A. J. Tholt, T. S. Tobin, M. Widdowson, S. Anantharaman, D. C. Dassarma, and J. A. Wilson Mantilla. 2022. New mammals from the Naskal intertrappean site and the age of India's earliest eutherians. Palaeogeography, Palaeoclimatology, Palaeoecology 591:110857.

Submitted April 25, 2022; revisions received August 15, 2022;
accepted August 18, 2022.
Handling Editor: Erin Maxwell.